Published in final edited form as:
Free Radic Biol Med. 2010 December 1; 49(11): 1655–1665. doi:10.1016/j.freeradbiomed.2010.08.025.

Mouse brain plasmalogens are targets for hypochlorous acid-mediated modification in vitro and in vivo

Andreas Üllen[a], **Günter Fauler**[b], **Harald Köfeler**[c], **Sabine Waltl**[a], **Christoph Nusshold**[a], **Eva Bernhart**[a], **Helga Reicher**[a], **Hans-Jörg Leis**[d], **Andrea Wintersperger**[a], **Ernst Malle**[a], and **Wolfgang Sattler**[a,*]

[a]Institute of Molecular Biology and Biochemistry, Center for Molecular Medicine, Medical University of Graz, 8010 Graz, Austria

[b]Clinical Institute of Medical and Chemical Laboratory Diagnostics, Medical University of Graz, 8010 Graz, Austria

[c]Center of Medical Research, Medical University of Graz, 8010 Graz, Austria

[d]Research Unit of Osteology and Analytical Mass Spectrometry, University Children's Hospital, Medical University of Graz, 8010 Graz, Austria

Abstract

Plasmalogens, 1-*O*-alk-1′-enyl-2-acyl-*sn*-glycerophospholipids, are significant constituents of cellular membranes and are essential for normal brain development. Plasmalogens, which contain a vinyl ether bond at the *sn*-1 position, are preferential targets for hypochlorous acid (HOCl), generated by myeloperoxidase (MPO) from H_2O_2 and chloride ions. Because MPO is implicated in neurodegeneration, this study pursued two aims: (i) to investigate the reactivity of mouse brain plasmalogens toward HOCl in vitro and (ii) to obtain in vivo evidence for MPO-mediated brain plasmalogen modification. Liquid chromatography coupled to hybrid linear ion trap–Fourier transform–ion cyclotron resonance mass spectrometry revealed plasmalogen modification in mouse brain lipid extracts at lower HOCl concentrations as observed for diacylphospholipids, resulting in the generation of 2-chloro fatty aldehydes and lysophospholipids. Lysophosphatidylethanolamine accumulation was transient, whereas lysophosphatidylcholine species containing saturated acyl residues remained stable. In vivo, a single, systemic endotoxin injection resulted in upregulation of cerebral MPO mRNA levels to a range comparable to that observed for tumor necrosis factor-α and cyclooxygenase-2. This inflammatory response was accompanied by a significant decrease in several brain plasmalogen species and concomitant in vivo generation of 2-chlorohexadecanal. The present findings demonstrate that activation of the MPO–H_2O_2–chloride system under neuroinflammatory conditions results in oxidative attack of the total cerebral plasmalogen pool. As this lipid class is indispensable for normal neuronal function, HOCl-mediated plasmalogen modification is likely to compromise normal synaptic transmission.

*Corresponding author. Fax: +43 316 380 9615. wolfgang.sattler@medunigraz.at.

Europe PMC Funders Author Manuscripts

Keywords

Chlorinative stress; Endotoxin; Hypochlorite; Lipotoxicity; Myeloperoxidase; Neuroinflammation; Free radicals

The mammalian brain is particularly sensitive toward oxidative damage, a result of the high oxygen demand and the high content of unsaturated lipids in the central nervous system (CNS) [1]. Potential sources of reactive species in the brain are mitochondria, amyloid-β peptides, redox-active iron, the NADPH-oxidase complex, and myeloperoxidase (MPO) [1–3]. MPO, a member of the heme peroxidase family, is present in the azurophilic granules of phagocytes, and H_2O_2-dependent oxidation of chloride ions to the powerful oxidant hypochlorous acid/hypochlorite ($HOCl/OCl^-$) is catalyzed by MPO. Under physiological conditions MPO-generated oxidants play an important role in killing invading pathogens, thereby contributing to host defense [3]. However, chronic activation of MPO results in elevated levels of reactive species, favoring chloramine formation, a modification potentially leading to tissue and/or organ injury [4–8]. Increasing evidence points toward MPO as a disease-amplifying enzyme in neurodegeneration [2]. In multiple sclerosis, MPO is present in microglia/macrophages at lesion sites [9,10] and cortical demyelination is associated with increased MPO activity [11,12].

Most of the lipid subclasses important for normal CNS function are targets for MPO-dependent modification reactions: phospholipids are subject to HOCl modification involving attacks on the double bonds of unsaturated fatty acyl residues and/or headgroup modification, leading to chlorohydrin and/or chloramine generation [13]. In addition, nitrogen-centered radicals, phosphatidylglycoaldehydes, and phosphonitriles originating from either ethanolamine or serine phospholipids can be formed [14,15]. Sphingomyelin modification by HOCl added as a reagent or generated by the MPO–H_2O_2–chloride system results in the formation of several chlorinated species with high lipotoxic potential toward neurons [16].

Plasmalogens are glycerophospholipids in which the *sn*-1 aliphatic chain (predominantly C16 or C18) is attached to the glycerol backbone by a vinyl ether bond [17] and are particularly sensitive lipid targets for HOCl attack. This reaction generates chlorinated fatty aldehydes and the corresponding remnant lysophospholipid. 2-Chlorohexadecanal (2-ClHDA) is generated by activated neutrophils [18,19] and monocytes [20] and is present in human atherosclerotic lesions [7] and ischemic/reperfused myocardium [21]. This chloro fatty aldehyde is a potent neutrophil chemoattractant [19] and a potent inhibitor of vasculoprotective nitric oxide synthase in endothelial cells [18].

Interference with plasmalogen synthesis results in deleterious phenotypes. Studies performed in a mouse model carrying a targeted deletion of the dihydroxyacetone–phosphate acyltransferase gene (resulting in the complete absence of ether phospholipids) revealed male infertility, defects in eye development, and cataract formation and optic nerve hypoplasia [17,22]. Plasmalogen deficiency has a major impact on membrane dynamics and trafficking [23] and results in impaired blood–testis barrier function due to defective intracellular trafficking of tight-junction-associated claudin-3 [24]. With regard to CNS

function plasmalogen deficiency results in severe and long-lasting developmental alterations of the cerebellum, indicating an important role for plasmalogens in brain development and function [25]. Decreased plasmalogen content is also linked to peroxisomal biogenesis disorders [26,27] and to neurodegenerative diseases such as Alzheimer disease [28–30]. In the former plasmalogen deficiency is due to a synthesis defect, whereas in the latter oxidative modifications were suggested to be causally involved. Independent of the mechanism, depletion of brain plasmalogens most probably results in disturbed neuronal function: in white matter plasmalogens contribute to the maintenance of axonal sheaths [31], and in gray matter plasmalogens are required for membrane fusion (e.g., during synaptic vesicle formation) [32].

The above-mentioned evidence implicates that MPO is present in brain tissue of multiple sclerosis and Alzheimer disease patients and that local activation of MPO might contribute to neuropathology apparently via plasmalogen modification. Therefore this study aimed to characterize the loss of plasmalogens and concomitant product formation in response to NaOCl in a complex matrix of mouse brain lipid extracts by electrospray ionization Fourier transform–ion cyclotron resonance–mass spectrometry (ESI FT–ICR–MS) and gas chromatography (GC)–MS analysis in vitro. In a second in vivo approach we sought to obtain evidence for MPO-mediated modification of brain plasmalogens in the CNS: during these studies mice received a single systemic injection of lipopolysaccharide (LPS) to induce neuroinflammation. In this mouse model the expression of brain inflammatory markers and the outcome of brain plasmalogen composition and formation of 2-ClHDA via the MPO–H_2O_2–chloride system was investigated.

Materials and methods

Materials

Hexadecanoic-2,4,6,8,10,12,14,16-$^{13}C_8$ acid sodium salt, hexadecanal dimethyl acetal, and pentafluorobenzyl hydroxylamine were purchased from Sigma Aldrich (Vienna, Austria). LPS from *Escherichia coli* (0111:B4) and sodium hypochlorite (NaOCl) solution were obtained from Sigma Aldrich. The concentration of NaOCl was determined spectrophotometrically at pH 12 (ε_{292} = 350 M^{-1} cm^{-1}). Silica gel 60 plates were from Merck (Darmstadt, Germany). Dispase from *Bacillus polymyxa* was from Gibco (Invitrogen, Vienna, Austria) and the Bradford protein assay was from Bio-Rad (Vienna, Austria). All other chemicals and solvents were from Sigma, Pierce (Vienna, Austria), and Roth (Vienna, Austria).

Modification of murine brain lipid extracts by NaOCl

Male C57BL/6 mice (8–10 weeks, 20–30 g) were obtained from the Institut für Versuchstierkunde (Himberg, Austria). Animals were killed by cervical dislocation, and brains were removed, snap-frozen in liquid N_2, and homogenized in a mortar. The powdered material was transferred to preweighed Pyrex tubes and extracted according to the Folch procedure [33]. Liposomes from brain lipids were prepared by dispersing 50 mg brain lipids in 1 ml H_2O using sonication (4×10 s on ice). Modification with NaOCl (1–500 μg/100 μg lipid) was performed at pH 7 overnight at room temperature (RT). Based on a percentage

brain lipid (lipid fraction contributes approx 10% of total wet brain tissue) composition of 65% total phospholipids, 11% total sphingolipids, and 20% cholesterol [34], these weight ratios correspond to molar NaOCl:lipid ratios of approx 0.1:1 (1 μg NaOCl/100 μg lipid) to 50:1 (500 μg NaOCl/100 μg lipid). Subsequently, lipids were extracted, dissolved in 1 ml $CHCl_3$/MeOH (1/1, v/v), and analyzed by FT–ICR–MS.

FT–ICR–MS

Analysis was performed on an Accela U-HPLC coupled to a LTQ-FT Ultra hybrid mass spectrometer (Thermo Scientific, Vienna, Austria). Samples were diluted (1:100) in chloroform/methanol (1/1, v/v). Either D-31 34:1 phosphatidylcholine (PC) or 12:0/12:0 PC and LIPID MAPS standards (Avanti Polar Lipids) LM-1004 (17:0/14:1 PC), LM-1102 (17:0/20:4 phosphatidylethanolamine; PE), LM-1303 (21:0/22:6 phosphatidylserine; PS), and LM-1504 (17:0/14:1 phosphatidylinositol; PI) were used as internal standards. Lipid samples were separated on a Thermo Hypersil Gold C18 column (100×1 mm, 1.9 μm particle size). Solvent A was water with 1% ammonium acetate and 0.1% formic acid. Solvent B was acetonitrile/2-propanol (5/2; v/v) with 1% ammonium acetate and 0.1% formic acid. The gradient ran from 35 to 70% B in 4 min and then to 100% B in another 16 min with a hold for an additional 10 min. The flow rate was 250 μl/min. Data acquisition was done by FT–ICR–MS full scan in preview mode, a resolution of 200 k, and <2 ppm mass accuracy with external calibration. The spray voltage was set to 5000 V, capillary voltage to 35 V, and the tube lens was at 120 V. Capillary temperature was at 250 °C. From the FT–ICR–MS preview scan the four most abundant *m/z* values were picked in data-dependent acquisition mode, fragmented in the linear ion trap analyzer, and ejected at nominal mass resolution. Normalized collision energy was set to 35%, the repeat count was 2, and the exclusion duration was 60 s.

Determination of 2-ClHDA stability in the presence of a mixed primary mouse brain cell suspension

Mouse brains were collected from animals killed by cervical dislocation. For each sample, 400 mg brain tissue was minced and supplemented to a final volume of 2 ml with HBSS (with 1 g/L glucose) containing 0.25 U dispase. After incubation for 90 min at 37 °C with stirring, enzymatic digestion was stopped by washing (120 *g*, 10 min, RT) the brain cell suspension three times with 2 ml HBSS (supplemented with 1 g/L glucose) containing 1 mM EDTA. Subsequently, 2 ml brain cell suspension was supplemented with 2-ClHDA (17 μg; 30 μM final concentration) and further incubated at 37 °C under gentle stirring. At the indicated time points 125 μl aliquots were removed, snap-frozen, and stored at −70 °C until analysis. 2-ClHDA was quantified in the presence of 0.75 μg 2-chloro-[2,4,6,8,10,12,14,16-$^{13}C_8$]-hexadecanal (2-Cl[$^{13}C_8$]HDA; see below). A one-phase exponential decay model ($A \times e^{-kt}$) was used to fit experimental data using Prism 5.0 software (GraphPad, San Diego, CA, USA).

Animal experiments

Animals experiments using C57BL/6 mice were performed in accordance with animal care ethics approval and guidelines, as per Animal Care Certificate BMWF-66.010/0104-II/10b/

2009 of the Austrian Federal Ministry of Science and Research (Vienna, Austria). All animals were kept on a 12-h light/dark cycle with free access to food and water. Neuroinflammation was induced by ip injection of a single dose of LPS (150 μg/30 g) and time-dependently monitored by quantitative real-time PCR (qPCR; see below). After the indicated time points mice were killed by cervical dislocation, and brains were removed, homogenized, and processed further for analysis.

qPCR

To generate cDNA templates, total brain RNA was isolated using a Paris Kit (Ambion, Brunn a. Gebirge, Austria) and 5 μg RNA was reverse transcribed according to the manufacturer's instructions using 200 U SuperScript II reverse transcriptase (Invitrogen) and random hexamer primers (Amersham Biosciences, Vienna, Austria). Primers for MPO were designed using NCBI Primer Blast. qPCR was performed with an Applied Biosystems 7900HT fast real-time PCR system, the QuantiFast SYBR Green PCR kit, and primer assays for tumor necrosis factor α (TNFα) , cyclooxygenase-2 (COX2), and TATA-box binding protein (TBP1; Table 1). Samples were run in triplicate for each experiment, with TBP1 as an internal control. For analysis of the expression profiles the public domain program Relative Expression Software Tool—REST 384 version 2 (http://www.gene-quantification.com/download.html) was used [35].

Measurement of MPO mass in murine brain homogenates

MPO protein mass was measured using a specific sandwich ELISA according to the manufacturer's recommendations (HK210 kit; Hycult Biotechnology, Uden, The Netherlands) and normalized on total protein content as determined by the Bradford assay.

Quantitation of 2-ClHDA by GC–MS

Synthesis of stable isotope-labeled 2-ClHDA—2-Cl[$^{13}C_8$]HDA and 2-ClHDA were synthesized and purified as previously described [36] with some modifications (Supplementary Fig. I). Briefly, 1 eq hexadecanoic-2,4,6,8,10,12,14,16-$^{13}C_8$ acid was reduced to hexadecanol-[2,4,6,8,10,12,14,16-$^{13}C_8$] by using 4 eq $LiAlH_4$ (refluxed at 50 °C overnight in dry diethyl ether; the reaction was quenched by addition of ethyl acetate and Milli-Q water). Hexadecanal-[2,4,6,8,10,12,14,16-$^{13}C_8$] was synthesized by partial oxidation of 1 eq hexadecanol-[2,4,6,8,10,12,14,16-$^{13}C_8$] in CH_2Cl_2 at −70 °C for 1 h under a stream of N_2 utilizing oxalyl chloride-activated dimethyl sulfoxide (DMSO; 3 eq oxalyl chloride and 6 eq DMSO) as a catalyst. The reaction mixture was quenched by the addition of 12 eq triethylamine, stirred for an additional 10 min, and allowed to warm at RT. After the reaction mixture was washed with Milli-Q water the organic phase was brought to dryness and converted to the dimethyl acetal derivative by addition of methanol:trimethyl orthoformate (90:10, v/v) and NH_4NO_3 and incubation for 48 h at 40 °C. Subsequently, hexadecanal-[2,4,6,8,10,12,14,16-$^{13}C_8$] dimethyl acetal (HDA-[$^{13}C_8$] dma) was purified using a Silica 60 column and hexane/diethyl ether (97.5/2.5, v/v) as eluent. For synthesis of 2-Cl[$^{13}C_8$]HDA dma, HDA-[$^{13}C_8$] dma in acetonitrile (1.25%, w/v) was added to a suspension of $MnCl_2$ (2.5%, w/v) and MnO_2 (2.5%, w/v). Then trimethylchlorosilane (10%, v/v) was added and the reaction mixture was heated to 40 °C. After 16 h, 0.5 M NaOH

(75%, v/v) was added for alkalization, and 2-Cl[$^{13}C_8$] HDA dma was extracted with hexane and purified using a Silica 60 column and hexane/diethyl ether (90/10, v/v) as eluent. For each experiment 2-Cl[$^{13}C_8$]HDA was freshly prepared by refluxing the dimethyl acetal derivative in trifluoroacetic acid/CH_2Cl_2 (1/1, v/v) at 80 °C for 1 h. Purity was confirmed by thin-layer chromatography (TLC), as well as by GC–MS of the corresponding pentafluorobenzyl (PFB) oxime derivative (see below). Synthetic 2-ClHDA was prepared and purified in a manner similar to that for the stable isotope-labeled compound except that hexadecanal dimethyl acetal (Sigma) was used as the starting compound.

Derivatization—2-ClHDA as well as lipid extracts from brain tissue was dissolved in 100 μl of ethanol, and 100 μl of a solution of PFB–hydroxylamine in ethanol (6 mg/ml, w/v) was added. After 1 h at 25 °C, 1 ml of distilled water was added, and the PFB–oxime derivative was extracted with hexane/diethyl ether (4/1, v/v) and dried under N_2. The samples were redissolved in 100 μl hexane, transferred to autosampler vials, and stored at −20 °C until GC–MS analysis.

Preseparation of brain lipid extracts by thin-layer chromatography—Lipid extracts from one brain (2.5 μg 2-Cl[$^{13}C_8$]HDA added as internal standard (I.S.)) were reconstituted in 500 μl $CHCl_3$ and fractionated on silica gel 60 plates using hexane/diethyl ether/acidic acid (90/10/1, v/v/v) as the mobile phase. Fractions comigrating with an authentic 2-ClHDA standard were scraped off, extracted from the TLC sorbent, converted to the corresponding PFB–oximes, and analyzed by GC–MS as described below.

GC–MS analysis—Samples were separated on a Thermo Scientific Trace GC Ultra (helium was used as carrier gas, 2 ml/min) with an SGE BPX5 capillary column (15 m, 0.25 mm inner diameter, 0.25 μm methyl silicone film coating) and analyzed using a DSQII mass spectrometer (Thermo Scientific, Waltham, MA, USA). Injector temperature was set to 230 °C and ion source temperature was 225 °C. The oven temperature was kept at 100 °C for 5 min, increased during the first ramping step at a rate of 20 °C/min to 175 °C, and held at 175 °C for 1 min. In the second ramping step the temperature was raised at a rate of 15 °C/min to 280 °C and held at 280 °C for an additional 2 min. All spectra were monitored in negative ion chemical ionization (NICI; methane was used as reagent gas), either in full scan mode or using selected ion monitoring at *m/z*=414 and *m/z*=288/290 (characteristic isotopic distribution of chlorine in the corresponding C16:0 chloro fatty aldehyde residue). Quantitation was performed by peak area comparison with the stable isotope-labeled standard (0.5 to 2.5 μg added per sample). 2-Chlorooctadecanal (*m/z*=316/318 and 442) and 2-chlorooctadecenal (*m/z*=314/316 and 440) were quantified using 2-Cl[$^{13}C_8$]HDA as internal standard.

Total plasmalogen aldehydes were quantified after acidic hydrolysis in 0.1 M HCl (overnight at RT), preparation of PFB–oxime derivatives, and subsequent NICI–GC–MS analysis using 2-Cl[$^{13}C_8$] HDA as internal standard.

Statistical analyses

Data are presented as means±SD or SEM. To test differences within groups, statistical significance was determined either by ANOVA and Dunnett test or (for qPCR data) by REST 38, version 2 [35]. All values of $p \leq 0.05$ were considered significant.

Results

Phospholipid composition of mouse brain lipids

In a first series of experiments the quantitative composition of the total mouse brain phospholipid pool was analyzed. The major contribution is provided by PC (37%), followed by PE (25%), plasmenyl PE (pPE; 23%), PS (12%), PI (3%), and plasmenyl PC (pPC; 0.2%; Fig. 1A). Next, the molecular species composition of these phospholipids was analyzed by FT–ICR–MS (Figs. 1B–E; the detailed composition including *m/z* values is displayed in Supplementary Table I). The predominant species within the PC family are 32:0, 34:1, and 36:1, accounting for approx 70% of total PC (Fig. 1B). In the pPC group 34:0 is the most abundant species (54%; Fig. 1C). Within the PE family 38:4 and 40:6 predominate (61%; Fig. 1D), whereas in the pPE cluster 36:1, 36:2, and 40:6 (43%; Fig. 1E) are the most abundant members. PI contains 63% of 38:4 and the major subspecies in PS is 40:6 (63%; Supplementary Fig. II).

Modification of phosphoethanolamines and phosphocholines in mouse brain lipids by NaOCl in vitro

Mouse brain lipid extracts were incubated with NaOCl at increasing mass ratios (for approx molar ratios see Materials and methods). FT–ICR–MS analyses revealed almost quantitative consumption of unsaturated pPE species at oxidant:lipid mass ratios ranging from 1:100 to 10:100 (Fig. 2A). In contrast, PE species were more resistant to HOCl treatment (Fig. 2B), with quantitative modification occurring at oxidant:lipid mass ratios ranging from 50:100 to 500:100. The corresponding remnant lyso-compounds (formed upon HOCl attack of the vinyl ether bond and subsequent abstraction of 2-chloroaldehydes from the *sn*-1 position; [7]) are detectable at oxidant:lipid ratios between 1:100 and 50:100 in a transient manner (Fig. 2C). Lysophospholipids containing an unsaturated *sn*-2 acyl residue (20:4 and 18:1; *m/z*=501.3 and 479.3, respectively) are less stable at higher oxidant:lipid ratios compared to their corresponding saturated counterparts (16:0 and 18:0; *m/z*=453.3 and 481.3). Comparable observations were made for pPC and PC subspecies: pPC species are modified at low oxidant:lipid ratios (Fig. 2D), whereas almost complete modification of PC species is observed only at higher HOCl concentrations (50:100 and 500:100; Fig. 2E). Approx 20% of the 32:0 and 34:0 species were still detectable at a fivefold NaOCl excess over lipids. With regard to lyso-PC formation the accumulation of the unsaturated 20:1 species is transient (*m/z*=549.4), whereas accumulation of the corresponding saturated lyso-PC compounds (16:0 and 18:0; *m/z*=495.3 and 523.4) occurs in a HOCl-dependent manner (Fig. 2F).

HOCl treatment of plasmalogens present in cellular membranes or lipoproteins gives rise to the formation of lysophospholipids and 2-chloro fatty aldehydes ([19,20]; Fig. 3A). To investigate whether this route is also relevant to the CNS, brain lipids were modified with

NaOCl. The decrease in selected plasmalogen species (the alkenyl residue at the *sn*-1 was identified by MS/MS experiments; *sn*-1=16:0, 18:0, and 18:1) was followed by FT–ICR–MS. In parallel, formation of 2-chloroaldehydes was quantified by GC–MS using 2-Cl[$^{13}C_8$]HDA as internal standard (outlined under Materials and methods). Supplementary Fig. III shows chromatograms and mass spectra of the PFB–oxime derivatives of 2-ClHDA (Fig. IIIA) and 2-Cl[$^{13}C_8$]HDA (Fig. IIIB) eluting at 14.97 min. Under our analytical conditions the molecular ions (M^-) at *m/z* 469 (PFB–oxime of 2-ClHDA) and 477 (PFB–oxime of 2-Cl[$^{13}C_8$]HDA) were detected in low abundance. The intensity ratio of the fragment ions observed at 288/290 (2-ClHDA) and 296/298 (2-Cl[$^{13}C_8$]HDA) of approx 3:1 is indicative of the presence of two chlorine isotopes ($^{35}Cl/^{37}Cl$) in the analyte. The additional fragment ions observed at *m/z* 414 (or 422 for 2-Cl[$^{13}C_8$]HDA), 196, and 181 are characteristic of the 2-ClHDA PFB–oxime derivatives [19].

In line with data shown in Fig. 2, pPE species containing 16:0, 18:0, and 18:1 at the *sn*-1 position were quantitatively modified at a oxidant:lipid ratio of 5:100 (Fig. 3B). In addition to 2-ClHDA we could detect other 2-chloro fatty aldehydes generated by HOCl attack of plasmalogen subspecies [37]. Depending on the alkenyl residue present in the *sn*-1 position either 2-chlorooctadecanal (from C18:0) or 2-chlorooctadecenal (from C18:1) was formed (Fig. 3C). The oxidant:lipid ratio at which the corresponding pPE species are quantitatively consumed (5:100) closely corresponds to the HOCl concentration at which maximal 2-chloroaldehyde yields were obtained (4.1, 3.3, and 1 μmol/g brain tissue for 2-ClHDA, 2-chlorooctadecenal, and 2-chlorooctadecanal, respectively; Fig. 3C). The next experiments were designed to compare the total fatty aldehyde content with the amount of chloroaldehydes formed after treatment of mouse brain lipid extracts with NaOCl. To analyze the total aldehyde content of mouse brain lipid extracts, plasmalogens were subjected to acidic hydrolysis (0.1 M HCl, RT, overnight), and the released aldehydes were converted to the PFB–oxime derivatives and then quantified by NICI–GC–MS (Fig. 3C). In a parallel set of experiments, brain lipids were modified with NaOCl and 2-chloro fatty aldehydes were quantified. These analyses revealed that 1-*O*-hexadecanal (C16:0) and 1-*O*-octadecenal (C18:1) plasmalogens were nearly quantitatively consumed by NaOCl, whereas only 15 to 20% of the corresponding 1-*O*-octadecanal (C18:0) plasmalogen was susceptible to HOCl attack (Fig. 3D).

To get an indication about the lifetime of 2-ClHDA in brain tissue, 2-ClHDA (17 μg) was incubated in the presence of a crude primary brain cell suspension and the 2-ClHDA content was time-dependently analyzed. By nonlinear regression analysis, the data shown in Fig. 4 were fitted using a one-phase exponential decay function. This curve fit revealed a *t*/2 of approx 40 min for 2-ClHDA in the presence of a mixed primary brain cell population. The inset in Fig. 4 shows potential decay pathways for 2-ClHDA.

Systemic LPS induces transcription of cerebral inflammatory markers

To follow the time course of neuroinflammation under in vivo conditions, transcriptional activation of MPO and two other inflammatory markers (TNFα and COX2) was analyzed by qPCR. Analyses in brains of LPS-treated mice revealed significantly elevated mRNA levels of all three markers (Fig. 5A). At the earliest time point (6 h) the highest induction was

observed for TNFα (ninefold), followed by MPO (fourfold) and COX2 (threefold). Thereafter TNFα and COX2 levels started to decline and MPO appeared to be induced in a second phase after 24 h. At the latest time point analyzed (72 h) COX2 levels returned to baseline values, whereas MPO and TNFα mRNA remained elevated. To get an indication of MPO protein levels, brain protein extracts were analyzed by ELISA. Systemic endotoxin application significantly increased MPO protein concentrations at 24 h post-application (Fig. 5B).

Systemic LPS affects brain plasmalogen levels and plasmalogen-derived oxidation products

To evaluate the outcome of neuroinflammatory conditions on plasmalogen levels in vivo, the brain plasmalogen composition of mice receiving a single systemic endotoxin injection was analyzed by FT–ICR–MS. Overall plasmalogen loss at 48 and 96 h post-LPS exposure accounted for approx 10 and 18% (Fig. 6A). For pPC species a slight but statistically significant decrease was observed for 34:1, 36:1, and 36:2 species but not for the most abundant 34:0 species (Fig. 6B). In contrast, in the pPE group significantly decreased levels of the 34:1, 36:1, 38:1, 38:4, 38:6, 40:4, 40:5, and 40:6 species were observed (Fig. 6C).

Because systemic LPS application is coupled to an increase in brain MPO mRNA and protein levels (Fig. 5) and is paralleled by loss of plasmalogen species (Fig. 6), oxidative modification via intermediate formation of HOCl is likely to occur. To confirm this, the accumulation of MPO-derived 2-ClHDA was quantified in brain lipid extracts of LPS-treated animals by NICI–GC–MS. Along this line it is important to note that during in vivo experiments we were unable to unambiguously identify 2-ClHDA when PFB–oxime derivatives were prepared directly from total brain lipid extracts. However, a preseparation of brain lipid extracts by TLC (to obtain an enriched 2-chloro fatty aldehyde fraction as described under Materials and methods) and subsequent GC–MS analysis of PFB–oxime derivatives clearly revealed the presence of 2-ClHDA in brain lipids of endotoxin-treated mice (Fig. 7).

Fig. 7A shows selected ion-monitoring traces of PFB–oxime derivatives of 2-ClHDA (analyzed from brain lipid extracts prepared 6 h post-LPS; diagnostic ions at *m/z*=288 and 290) and 2-Cl[$^{13}C_8$] HDA (*m/z* = 296 and 298) used as internal standard. Ion intensity ratios are close to 3:1 as expected for a chlorinated analyte (Fig. 7B). Quantitative data for time-dependent 2-ClHDA generation in brains of LPS-treated mice are shown in Fig. 7C. Under the conditions applied during these in vivo experiments 2-ClHDA concentrations remained significantly elevated over baseline levels for 48 h post-LPS injection.

Discussion

Findings of this study strengthen the concept that chlorinative stress is implicated in neurodegeneration [2]. In particular we demonstrate that brain plasmalogens, which are essential for the normal function of the CNS [17], are targeted by MPO-derived HOCl, resulting in the production of 2-chloro fatty aldehydes and the corresponding lysophospholipids. Both compound classes have potent cytotoxic properties.

Plasmalogens, major constituents of neural tissue, can contribute between 50 and 80% of total glycerophosphoethanolamines in gray and white matter, respectively [28]. This is consistent with findings of this study in that PE and pPE were present in almost equimolar amounts, whereas the pPC content in mouse brain is minute and below 0.5 mol%. With regard to subspecies composition pPE are mostly unsaturated, with saturated species contributing ≈2%. This is in agreement with published data [28,38,39] and most likely a reflection of pPE function: species with a low degree of unsaturation are present in white matter myelin, providing support for axonal membrane integrity [31]. The highly unsaturated species are mainly found in gray matter, where they promote membrane fusion [40] and provide a reservoir for plasmalogen-specific phospholipase that generates bioactive signaling lipids [41].

The rate constants for HOCl-dependent plasmalogen modification are approx 10-fold higher compared to their non-vinyl ether-containing counterparts [42]. Accordingly, our in vitro data obtained during HOCl modification revealed higher sensitivity of brain plasmalogens toward HOCl compared to diacylglycerophospholipids. The polar headgroup of pPE is also subject to HOCl or HOBr attack, leading to the formation of halamines, which are able to induce oxidation of a plasmalogen model compound, albeit chloramines have a much slower oxidation kinetics than the corresponding bromamines [42]. In addition protein-derived chloramines are able to initiate secondary plasmalogen modification: The most potent are histidine chloramine analogues (with reaction kinetics only 5- to 30-fold slower than HOCl), whereas *N*-acetyllysine and taurine chloramines are less effective (approx 10^5-fold slower than HOCl [42,43]).

The decrease in plasmalogen species was accompanied by accumulation of lysophospholipids and the corresponding 2-chloroaldehydes derived from the *sn*-1 vinyl ether group. The observed transient accumulation of lysophospholipids in response to HOCl treatment is most likely a result of secondary modification reactions occurring at the remnant lysophospholipid, where chloramine formation at the ethanolamine headgroup [44], chlorohydrin formation in the alkene side chains [13], or *sn*-2 acyl abstraction [45,46] may be involved.

The second part of our study aimed to corroborate in vitro data in an in vivo mouse model of neuroinflammation using a single systemic LPS injection. This treatment regimen causes progressive loss of neurons in the substantia nigra in male mice [47]. Under normal conditions peripheral LPS passage across the blood–brain barrier is low [48] and therefore does not induce brain inflammation directly. However, systemic LPS induces hepatic TNFα synthesis and secretion and subsequent TNFα-receptor-dependent signal transduction to the brain, where TNFα synthesis is further amplified [49]. This creates a milieu of persistent and self-propelling neuroinflammation, a scenario in which bioactive lipids (e.g., lysophospholipids or prostaglandins formed via COX2) take a central regulatory role [50]. During our study we observed a biphasic increase in MPO mRNA levels and a transient increase in MPO protein. This might be the result of a superimposition of transcriptional regulation and import of mature MPO into the brain, which is comparable to findings reported for a murine stroke model: there, MPO-positive neutrophils were detected at days 1 and 3, whereas MPO-positive macrophages/microglia were detected at later stages up to 3

weeks post-stroke induction [51]. This raises the question about the origin of cerebral MPO: multiple resident cell types such as astrocytes [52], microglia [53], and neurons [54] were reported to contain and/or express MPO. Alternatively, MPO could be imported by invading neutrophils or monocytes [51,55]. Independent of the source of cerebral MPO it was shown that $MPO^{-/-}$ mice are more resistant to MPTP-induced neurotoxicity than their wild-type littermates, a fact reflected by decreased loss of neurons in the substantia nigra of $MPO^{-/-}$ animals [52]. On the other hand, astrocyte-specific overexpression of human MPO in an Alzheimer disease mouse model resulted in cognitive decline and accumulation of the lipid peroxidation product 4-hydroxynonenal along with the formation of phospholipid- and plasmalogen-derived hydro(pero)xides [56].

We have detected substantial amounts of 2-ClHDA (2 μg/g wet brain containing approx 80% water resulting in a concentration of approx 10 μM) only in endotoxin-injected mice. These 2-ClHDA concentrations are in a range comparable to that reported for a rat model of myocardial infarction (approx 1 μM [21]) and for human atherosclerotic lesion material (approx 10 μM [7]). This provides clear evidence that MPO-dependent plasmalogen modification is a neuroinflammatory event.

Our in vitro and in vivo data permit a rough estimation of MPO-mediated events contributing to overall plasmalogen loss: The cerebral concentration of 1-*O*-hexadecenyl plasmalogens is about 4 μmol/g tissue (Fig. 3C); plasmalogen loss 96 h post-LPS exposure is approx 20% (Figs. 6A and C), corresponding to an overall loss of approx 800 nmol/g tissue of 1-*O*-hexadecenyl-containing plasmalogens. Maximal concentration of 2-ClHDA was 2 μg/g brain (Fig. 7C), equivalent to 7.3 nmol 2-ClHDA/g tissue. Thus, MPO-dependent 2-ClHDA formation accounts for roughly 1% of total cerebral plasmalogen loss in vivo. However, this might be an underestimation: in vitro incubation of 2-ClHDA in the presence of a mixed primary brain cell suspension revealed a *t*/2 of approx 40 min for 2-ClHDA (Fig. 4). This could result from further metabolism of 2-ClHDA by fatty aldehyde dehydrogenase (FALDH) [57]. FALDH (classified as ALDH3A2; SwissProt P51648) is expressed in brain and when mutated or absent causes severe neurological symptoms [58]. Alternatively, oxidation of 2-ClHDA to 2-chlorohexadecanoic acid and subsequent incorporation into the polar lipid fraction could redirect 2-ClHDA via 2-chlorohexadecanoic acid into an inert and stable storage pool [59]. Finally, Schiff base formation between 2-chloro fatty aldehydes and ethanolamine-containing glycerophospholipids and/or the ε-amino group of protein lysine residues [60,61] could account for the observed time-dependent decrease in cerebral 2-ClHDA concentrations (Fig. 4, inset). The fact that rodent MPO activity is about 5–10 times lower compared to that of human phagocytes [62,63] indicates that the contribution of MPO to plasmalogen degradation could be substantially higher in humans.

Our data further indicate that MPO-dependent modification reactions contribute to but might not represent the only trigger for brain plasmalogen deficiency under neuroinflammatory conditions. This is supported by the fact that glycerol-3-phosphate-*O*-acyltransferase, a key enzyme in plasmalogen biosynthesis, is significantly down-regulated by TNFα (which was significantly upregulated during this study; Fig. 5) under in vitro and in vivo conditions [64,65]. Activation of a plasmalogen-specific phospholipase could be another factor contributing to plasmalogen loss under inflammatory conditions [41].

In conclusion, decreased plasmalogen content was reported for several neuropathological conditions including Alzheimer disease [30,66], Gaucher's disease [67], Down syndrome [68], a double knockout (Pex7 and Abcd1) mouse model resembling peroxisomal disorders [27], or experimental autoimmune encephalomyelitis [65]. Independent of the mechanism of plasmalogen loss, i.e., impaired synthesis or increased degradation/modification, the outcome for nervous system function is dismal. Results obtained during this study provide a potential framework on which, after elicitation of the systemic inflammatory response and propagation to the central nervous system, MPO-derived chlorinating species could oxidatively damage brain plasmalogens and thus exacerbate neuropathological conditions.

Supplementary Material

Refer to Web version on PubMed Central for supplementary material.

Acknowledgments

Financial support was provided by the Austrian Science Fund (Grants F3007 and P19074-B05) and the Austrian Research Promotion Agency (Grant No. Bridge P810994). C.N. was funded by the Ph.D. program Molecular Medicine of the Medical University of Graz, A.Ü. and S.W. are funded by the Austrian Science Fund within the Ph.D. program Molecular Medicine of the Medical University of Graz.

References

[1]. Halliwell B. Oxidative stress and neurodegeneration: where are we now? J. Neurochem. 2006; 97:1634–1658. [PubMed: 16805774]

[2]. Yap YW, Whiteman M, Cheung NS. Chlorinative stress: an under appreciated mediator of neurodegeneration? Cell. Signal. 2007; 19:219–228. [PubMed: 16959471]

[3]. Klebanoff SJ. Myeloperoxidase: friend and foe. J. Leukoc. Biol. 2005; 77:598–625. [PubMed: 15689384]

[4]. Hazell LJ, Arnold L, Flowers D, Waeg G, Malle E, Stocker R. Presence of hypochlorite-modified proteins in human atherosclerotic lesions. J. Clin. Invest. 1996; 97:1535–1544. [PubMed: 8617887]

[5]. Malle E, Waeg G, Schreiber R, Grone EF, Sattler W, Grone HJ. Immunohistochemical evidence for the myeloperoxidase/H_2O_2/halide system in human atherosclerotic lesions: colocalization of myeloperoxidase and hypochlo-rite-modified proteins. Eur. J. Biochem. 2000; 267:4495–4503. [PubMed: 10880973]

[6]. Grone HJ, Grone EF, Malle E. Immunohistochemical detection of hypochlorite-modified proteins in glomeruli of human membranous glomerulonephritis. Lab. Invest. 2002; 82:5–14. [PubMed: 11796821]

[7]. Thukkani AK, McHowat J, Hsu FF, Brennan ML, Hazen SL, Ford DA. Identification of alpha-chloro fatty aldehydes and unsaturated lysophosphatidylcholine molecular species in human atherosclerotic lesions. Circulation. 2003; 108:3128–3133. [PubMed: 14638540]

[8]. Rudolph V, Andrie RP, Rudolph TK, Friedrichs K, Klinke A, Hirsch-Hoffmann B, Schwoerer AP, Lau D, Fu X, Klingel K, Sydow K, Didie M, Seniuk A, von Leitner EC, Szoecs K, Schrickel JW, Treede H, Wenzel U, Lewalter T, Nickenig G, Zimmermann WH, Meinertz T, Boger RH, Reichenspurner H, Freeman BA, Eschenhagen T, Ehmke H, Hazen SL, Willems S, Baldus S. Myeloperoxidase acts as a profibrotic mediator of atrial fibrillation. Nat. Med. 2010; 16:470–474. [PubMed: 20305660]

[9]. Nagra RM, Becher B, Tourtellotte WW, Antel JP, Gold D, Paladino T, Smith RA, Nelson JR, Reynolds WF. Immunohistochemical and genetic evidence of myeloperoxidase involvement in multiple sclerosis. J. Neuroimmunol. 1997; 78:97–107. [PubMed: 9307233]

[10]. Chen JW, Breckwoldt MO, Aikawa E, Chiang G, Weissleder R. Myeloperoxidase-targeted imaging of active inflammatory lesions in murine experimental autoimmune encephalomyelitis. Brain. 2008; 131:1123–1133. [PubMed: 18234693]

[11]. Gray E, Thomas TL, Betmouni S, Scolding N, Love S. Elevated activity and microglial expression of myeloperoxidase in demyelinated cerebral cortex in multiple sclerosis. Brain Pathol. 2008; 18:86–95. [PubMed: 18042261]

[12]. Marik C, Felts PA, Bauer J, Lassmann H, Smith KJ. Lesion genesis in a subset of patients with multiple sclerosis: a role for innate immunity? Brain. 2007; 130:2800–2815. [PubMed: 17956913]

[13]. Spickett CM. Chlorinated lipids and fatty acids: an emerging role in pathology. Pharmacol. Ther. 2007; 115:400–409. [PubMed: 17658610]

[14]. Kawai Y, Kiyokawa H, Kimura Y, Kato Y, Tsuchiya K, Terao J. Hypochlorous acid-derived modification of phospholipids: characterization of aminophospholipids as regulatory molecules for lipid peroxidation. Biochemistry. 2006; 45:14201–14211. [PubMed: 17115715]

[15]. Flemmig J, Spalteholz H, Schubert K, Meier S, Arnhold J. Modification of phosphatidylserine by hypochlorous acid. Chem. Phys. Lipids. 2009; 161:44–50. [PubMed: 19577554]

[16]. Nusshold C, Kollroser M, Kofeler H, Rechberger G, Reicher H, Ullen A, Bernhart E, Waltl S, Kratzer I, Hermetter A, Hackl H, Trajanoski Z, Hrzenjak A, Malle E, Sattler W. Hypochlorite modification of sphingomyelin generates chlorinated lipid species that induce apoptosis and proteome alterations in dopaminergic PC12 neurons in vitro. Free Radic. Biol. Med. 2010; 48:1588–1600. [PubMed: 20226853]

[17]. Gorgas K, Teigler A, Komljenovic D, Just WW. The ether lipid-deficient mouse: tracking down plasmalogen functions. Biochim. Biophys. Acta. 2006; 1763:1511–1526. [PubMed: 17027098]

[18]. Marsche G, Heller R, Fauler G, Kovacevic A, Nuszkowski A, Graier W, Sattler W, Malle E. Chlorohexadecanal derived from hypochlorite-modified high-density lipoprotein-associated plasmalogen is a natural inhibitor of endothelial nitric oxide biosynthesis. Arterioscler. Thromb. Vasc. Biol. 2004; 24:2302–2306. [PubMed: 15514213]

[19]. Thukkani AK, Hsu FF, Crowley JR, Wysolmerski RB, Albert CJ, Ford DA. Reactive chlorinating species produced during neutrophil activation target tissue plasmalogens: production of the chemoattractant, 2-chlorohexadecanal. J. Biol. Chem. 2002; 277:3842–3849. [PubMed: 11724792]

[20]. Thukkani AK, Albert CJ, Wildsmith KR, Messner MC, Martinson BD, Hsu FF, Ford DA. Myeloperoxidase-derived reactive chlorinating species from human monocytes target plasmalogens in low density lipoprotein. J. Biol. Chem. 2003; 278:36365–36372. [PubMed: 12869568]

[21]. Thukkani AK, Martinson BD, Albert CJ, Vogler GA, Ford DA. Neutrophil-mediated accumulation of 2-ClHDA during myocardial infarction: 2-ClHDA-mediated myocardial injury. Am. J. Physiol. Heart Circ. Physiol. 2005; 288:H2955–H2964. [PubMed: 15681699]

[22]. Rodemer C, Thai TP, Brugger B, Kaercher T, Werner H, Nave KA, Wieland F, Gorgas K, Just WW. Inactivation of ether lipid biosynthesis causes male infertility, defects in eye development and optic nerve hypoplasia in mice. Hum. Mol. Genet. 2003; 12:1881–1895. [PubMed: 12874108]

[23]. Thai TP, Rodemer C, Jauch A, Hunziker A, Moser A, Gorgas K, Just WW. Impaired membrane traffic in defective ether lipid biosynthesis. Hum. Mol. Genet. 2001; 10:127–136. [PubMed: 11152660]

[24]. Komljenovic D, Sandhoff R, Teigler A, Heid H, Just WW, Gorgas K. Disruption of blood–testis barrier dynamics in ether-lipid-deficient mice. Cell Tissue Res. 2009; 337:281–299. [PubMed: 19495798]

[25]. Teigler A, Komljenovic D, Draguhn A, Gorgas K, Just WW. Defects in myelination, paranode organization and Purkinje cell innervation in the ether lipid-deficient mouse cerebellum. Hum. Mol. Genet. 2009; 18:1897–1908. [PubMed: 19270340]

[26]. Steinberg SJ, Dodt G, Raymond GV, Braverman NE, Moser AB, Moser HW. Peroxisome biogenesis disorders. Biochim. Biophys. Acta. 2006; 1763:1733–1748. [PubMed: 17055079]

[27]. Brites P, Mooyer PA, El Mrabet L, Waterham HR, Wanders RJ. Plasmalogens participate in very-long-chain fatty acid-induced pathology. Brain. 2009; 132:482–492. [PubMed: 19022859]

[28]. Han X, Holtzman DM, McKeel DW Jr. Plasmalogen deficiency in early Alzheimer's disease subjects and in animal models: molecular characterization using electrospray ionization mass spectrometry. J. Neurochem. 2001; 77:1168–1180. [PubMed: 11359882]

[29]. Han X. Potential mechanisms contributing to sulfatide depletion at the earliest clinically recognizable stage of Alzheimer's disease: a tale of shotgun lipidomics. J. Neurochem. 2007; 103(Suppl. 1):171–179. [PubMed: 17986152]

[30]. Ginsberg L, Rafique S, Xuereb JH, Rapoport SI, Gershfeld NL. Disease and anatomic specificity of ethanolamine plasmalogen deficiency in Alzheimer's disease brain. Brain Res. 1995; 698:223–226. [PubMed: 8581486]

[31]. Han XL, Gross RW. Plasmenylcholine and phosphatidylcholine membrane bilayers possess distinct conformational motifs. Biochemistry. 1990; 29:4992–4996. [PubMed: 2364071]

[32]. Glaser PE, Gross RW. Plasmenylethanolamine facilitates rapid membrane fusion: a stopped-flow kinetic investigation correlating the propensity of a major plasma membrane constituent to adopt an HII phase with its ability to promote membrane fusion. Biochemistry. 1994; 33:5805–5812. [PubMed: 8180209]

[33]. Folch J, Lees M, Sloane Stanley GH. A simple method for the isolation and purification of total lipides from animal tissues. J. Biol. Chem. 1957; 226:497–509. [PubMed: 13428781]

[34]. O'Brien JS, Sampson EL. Lipid composition of the normal human brain: gray matter, white matter, and myelin. J. Lipid Res. 1965; 6:537–544. [PubMed: 5865382]

[35]. Pfaffl MW, Horgan GW, Dempfle L. Relative expression software tool (REST) for group-wise comparison and statistical analysis of relative expression results in real-time PCR. Nucleic Acids Res. 2002; 30:e36. [PubMed: 11972351]

[36]. Albert CJ, Crowley JR, Hsu FF, Thukkani AK, Ford DA. Reactive chlorinating species produced by myeloperoxidase target the vinyl ether bond of plasmalogens: identification of 2-chlorohexadecanal. J. Biol. Chem. 2001; 276:23733–23741. [PubMed: 11301330]

[37]. Messner MC, Albert CJ, Hsu FF, Ford DA. Selective plasmenylcholine oxidation by hypochlorous acid: formation of lysophosphatidylcholine chlorohydrins. Chem. Phys. Lipids. 2006; 144:34–44. [PubMed: 16859663]

[38]. Yang K, Zhao Z, Gross RW, Han X. Shotgun lipidomics identifies a paired rule for the presence of isomeric ether phospholipid molecular species. PLoS ONE. 2007; 2:e1368. [PubMed: 18159251]

[39]. Taguchi R, Ishikawa M. Precise and global identification of phospholipid molecular species by an Orbitrap mass spectrometer and automated search engine Lipid Search. J. Chromatogr. A. 2010; 1217:4229–4239. [PubMed: 20452604]

[40]. Glaser PE, Gross RW. Rapid plasmenylethanolamine-selective fusion of membrane bilayers catalyzed by an isoform of glyceraldehyde-3-phosphate dehydrogenase: discrimination between glycolytic and fusogenic roles of individual isoforms. Biochemistry. 1995; 34:12193–12203. [PubMed: 7547960]

[41]. Farooqui AA. Studies on plasmalogen-selective phospholipase A(2) in brain. Mol. Neurobiol. 2010; 41:267–273. [PubMed: 20049656]

[42]. Skaff O, Pattison DI, Davies MJ. The vinyl ether linkages of plasmalogens are favored targets for myeloperoxidase-derived oxidants: a kinetic study. Biochemistry. 2008; 47:8237–8245. [PubMed: 18605737]

[43]. Pattison DI, Davies MJ. Kinetic analysis of the role of histidine chloramines in hypochlorous acid mediated protein oxidation. Biochemistry. 2005; 44:7378–7387. [PubMed: 15882077]

[44]. Richter G, Schober C, Suss R, Fuchs B, Birkemeyer C, Schiller J. Comparison of the positive and negative ion electrospray ionization and matrix-assisted laser desorption ionization-time-of-flight mass spectra of the reaction products of phosphatidylethanolamines and hypochlorous acid. Anal. Biochem. 2008; 376:157–159. [PubMed: 18295587]

[45]. Lessig J, Schiller J, Arnhold J, Fuchs B. Hypochlorous acid-mediated generation of glycerophosphocholine from unsaturated plasmalogen glycerophosphocholine lipids. J. Lipid Res. 2007; 48:1316–1324. [PubMed: 17395985]

[46]. Panasenko OM, Spalteholz H, Schiller J, Arnhold J. Myeloperoxidase-induced formation of chlorohydrins and lysophospholipids from unsaturated phosphatidylcholines. Free Radic. Biol. Med. 2003; 34:553–562. [PubMed: 12614844]

[47]. Liu Y, Qin L, Wilson B, Wu X, Qian L, Granholm AC, Crews FT, Hong JS. Endotoxin induces a delayed loss of TH-IR neurons in substantia nigra and motor behavioral deficits. Neurotoxicology. 2008; 29:864–870. [PubMed: 18471886]

[48]. Banks WA, Robinson SM. Minimal penetration of lipopolysaccharide across the murine blood–brain barrier. Brain Behav. Immun. 2010; 24:102–109. [PubMed: 19735725]

[49]. Qin L, Wu X, Block ML, Liu Y, Breese GR, Hong JS, Knapp DJ, Crews FT. Systemic LPS causes chronic neuroinflammation and progressive neurodegeneration. Glia. 2007; 55:453–462. [PubMed: 17203472]

[50]. Farooqui AA, Horrocks LA, Farooqui T. Modulation of inflammation in brain: a matter of fat. J. Neurochem. 2007; 101:577–599. [PubMed: 17257165]

[51]. Breckwoldt MO, Chen JW, Stangenberg L, Aikawa E, Rodriguez E, Qiu S, Moskowitz MA, Weissleder R. Tracking the inflammatory response in stroke in vivo by sensing the enzyme myeloperoxidase. Proc. Natl Acad. Sci. USA. 2008; 105:18584–18589. [PubMed: 19011099]

[52]. Choi DK, Pennathur S, Perier C, Tieu K, Teismann P, Wu DC, Jackson-Lewis V, Vila M, Vonsattel JP, Heinecke JW, Przedborski S. Ablation of the inflammatory enzyme myeloperoxidase mitigates features of Parkinson's disease in mice. J. Neurosci. 2005; 25:6594–6600. [PubMed: 16014720]

[53]. Reynolds WF, Rhees J, Maciejewski D, Paladino T, Sieburg H, Maki RA, Masliah E. Myeloperoxidase polymorphism is associated with gender specific risk for Alzheimer's disease. Exp. Neurol. 1999; 155:31–41. [PubMed: 9918702]

[54]. Green PS, Mendez AJ, Jacob JS, Crowley JR, Growdon W, Hyman BT, Heinecke JW. Neuronal expression of myeloperoxidase is increased in Alzheimer's disease. J. Neurochem. 2004; 90:724–733. [PubMed: 15255951]

[55]. Ji KA, Yang MS, Jeong HK, Min KJ, Kang SH, Jou I, Joe EH. Resident microglia die and infiltrated neutrophils and monocytes become major inflammatory cells in lipopolysaccharide-injected brain. Glia. 2007; 55:1577–1588. [PubMed: 17823975]

[56]. Maki RA, Tyurin VA, Lyon RC, Hamilton RL, DeKosky ST, Kagan VE, Reynolds WF. Aberrant expression of myeloperoxidase in astrocytes promotes phospholipid oxidation and memory deficits in a mouse model of Alzheimer disease. J. Biol. Chem. 2009; 284:3158–3169. [PubMed: 19059911]

[57]. Anbukumar DS, Shornick LP, Albert CJ, Steward MM, Zoeller RA, Neumann WL, Ford DA. Chlorinated lipid species in activated human neutrophils: lipid metabolites of 2-chlorohexadecanal. J. Lipid Res. 2010; 51:1085–1092. [PubMed: 20019386]

[58]. Rizzo WB, Carney G. Sjogren–Larsson syndrome: diversity of mutations and polymorphisms in the fatty aldehyde dehydrogenase gene (ALDH3A2). Hum. Mutat. 2005; 26:1–10. [PubMed: 15931689]

[59]. Wildsmith KR, Albert CJ, Anbukumar DS, Ford DA. Metabolism of myeloperoxidase-derived 2-chlorohexadecanal. J. Biol. Chem. 2006; 281:16849–16860. [PubMed: 16611638]

[60]. Wildsmith KR, Albert CJ, Hsu FF, Kao JL, Ford DA. Myeloperoxidase-derived 2-chlorohexadecanal forms Schiff bases with primary amines of ethanolamine glycerophospholipids and lysine. Chem. Phys. Lipids. 2006; 139:157–170. [PubMed: 16417904]

[61]. Stadelmann-Ingrand S, Pontcharraud R, Fauconneau B. Evidence for the reactivity of fatty aldehydes released from oxidized plasmalogens with phosphatidylethanolamine to form Schiff base adducts in rat brain homogenates. Chem. Phys. Lipids. 2004; 131:93–105. [PubMed: 15210368]

[62]. Rausch PG, Moore TG. Granule enzymes of polymorphonuclear neutrophils: a phylogenetic comparison. Blood. 1975; 46:913–919. [PubMed: 173439]

[63]. Noguchi N, Nakano K, Aratani Y, Koyama H, Kodama T, Niki E. Role of myeloperoxidase in the neutrophil-induced oxidation of low density lipoprotein as studied by myeloperoxidase-knockout mouse. J. Biochem. 2000; 127:971–976. [PubMed: 10833264]

[64]. Cimini A, Bernardo A, Cifone MG, Di Marzio L, Di Loreto S. TNFalpha downregulates PPARdelta expression in oligodendrocyte progenitor cells: implications for demyelinating diseases. Glia. 2003; 41:3–14. [PubMed: 12465041]

[65]. Singh I, Paintlia AS, Khan M, Stanislaus R, Paintlia MK, Haq E, Singh AK, Contreras MA. Impaired peroxisomal function in the central nervous system with inflammatory disease of experimental autoimmune encephalomyelitis animals and protection by lovastatin treatment. Brain Res. 2004; 1022:1–11. [PubMed: 15353207]

[66]. Goodenowe DB, Cook LL, Liu J, Lu Y, Jayasinghe DA, Ahiahonu PW, Heath D, Yamazaki Y, Flax J, Krenitsky KF, Sparks DL, Lerner A, Friedland RP, Kudo T, Kamino K, Morihara T, Takeda M, Wood PL. Peripheral ethanolamine plasmalogen deficiency: a logical causative factor in Alzheimer's disease and dementia. J. Lipid Res. 2007; 48:2485–2498. [PubMed: 17664527]

[67]. Moraitou M, Dimitriou E, Zafeiriou D, Reppa C, Marinakis T, Sarafidou J, Michelakakis H. Plasmalogen levels in Gaucher disease. Blood Cells Mol. Dis. 2008; 41:196–199. [PubMed: 18501647]

[68]. Murphy EJ, Schapiro MB, Rapoport SI, Shetty HU. Phospholipid composition and levels are altered in Down syndrome brain. Brain Res. 2000; 867:9–18. [PubMed: 10837793]

Europe PMC Funders Author Manuscripts

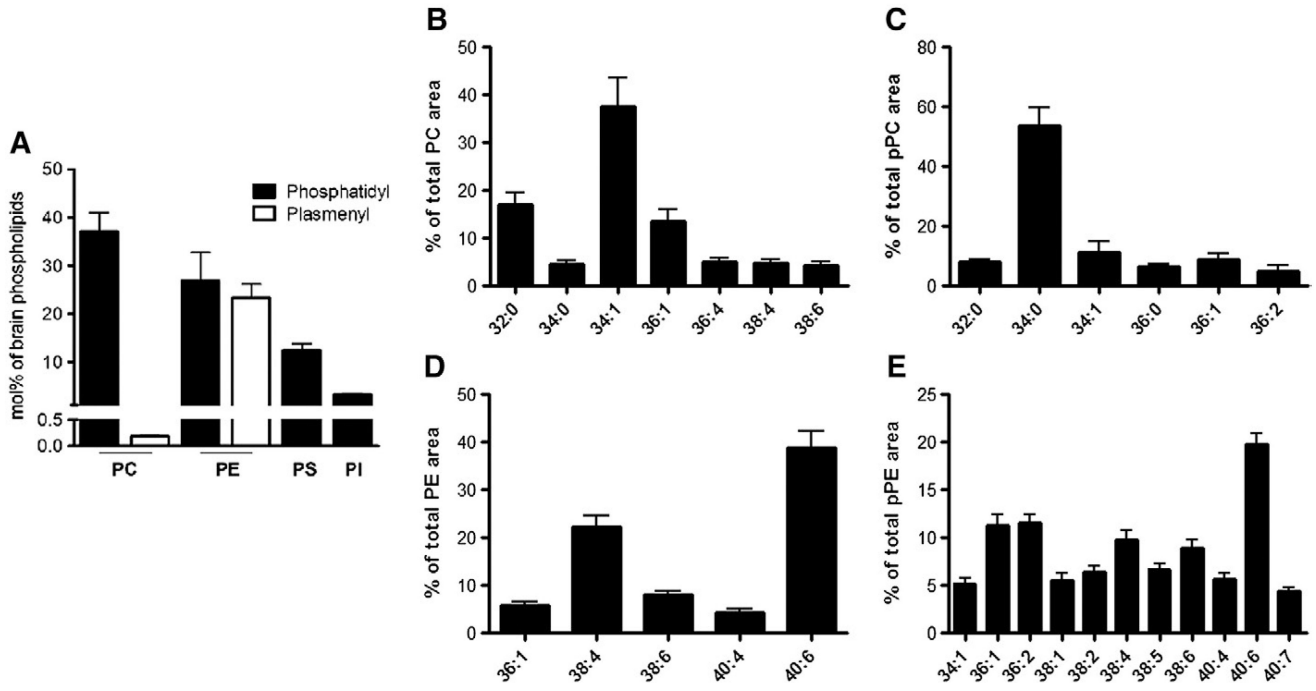

Fig. 1. FT–ICR–MS analyses of total murine brain glycerophospholipids.

C57BL/6 mice were killed by cervical dislocation, brains were removed and homogenized in liquid N_2, and lipids were extracted (twice) using a modified Folch extraction, dried under N_2, redissolved in $CHCl_3$/MeOH (1/1, v/v), and analyzed by a hybrid linear ion trap FT–ICR–MS in positive or negative (PI) ESI mode as described under Materials and methods. The corresponding *m/z* values and detailed percentage composition are given in Supplementary Table I. (A) Mol % composition of the total murine brain glycerophospholipids fraction. Internal standards were used as outlined under Materials and methods. (B–E) Molecular subspecies composition of (B) PC, (C) pPC, (D) PE, and (E) pPE of murine brain lipid extracts are shown. Only molecular species contributing >4% of total area are shown. Data shown represent means±SD from three mouse brains.

Europe PMC Funders Author Manuscripts

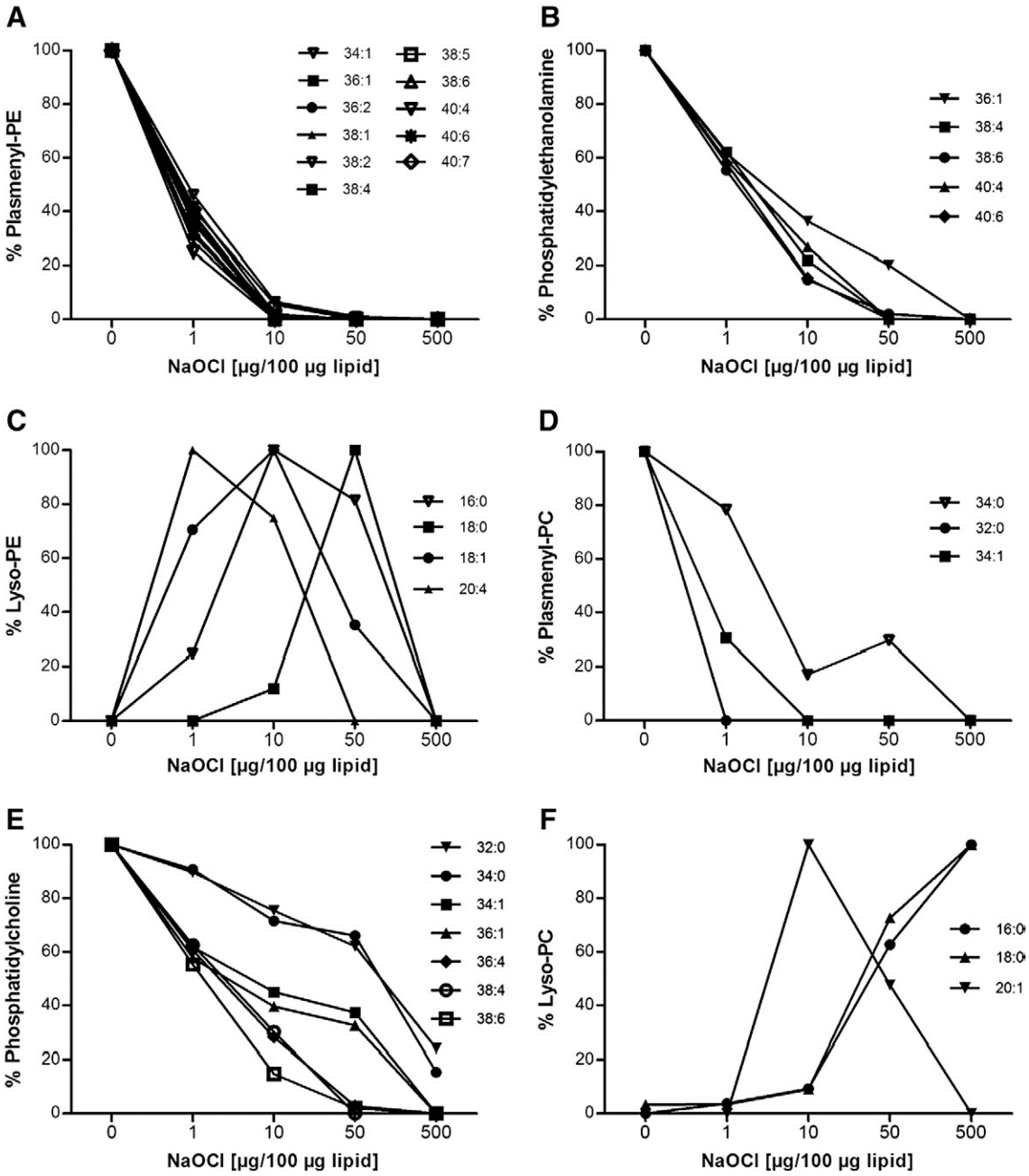

Fig. 2. Brain 1-*O*-alkenyl-2-acylglycerophospholipids are more sensitive toward NaOCl modification than their diacylglycerophospholipid counterparts in vitro.

Brain lipid extracts were prepared as described for Fig. 1 and modified at the indicated NaOCl concentrations at RT for 16 h. Analysis was performed by FT–ICR–MS in the positive ESI mode. (A–C) Effects of increasing HOCl:lipid ratios on the composition of pPE, PE, and lyso-PE. Oxidant:lipid ratio is given in terms of w/w. (D–F) Effects of increasing HOCl:lipid ratios on the composition of pPC, PC, and lysoPC. Oxidant:lipid ratio is given in terms of w/w. Results are mean values of duplicate determinations.

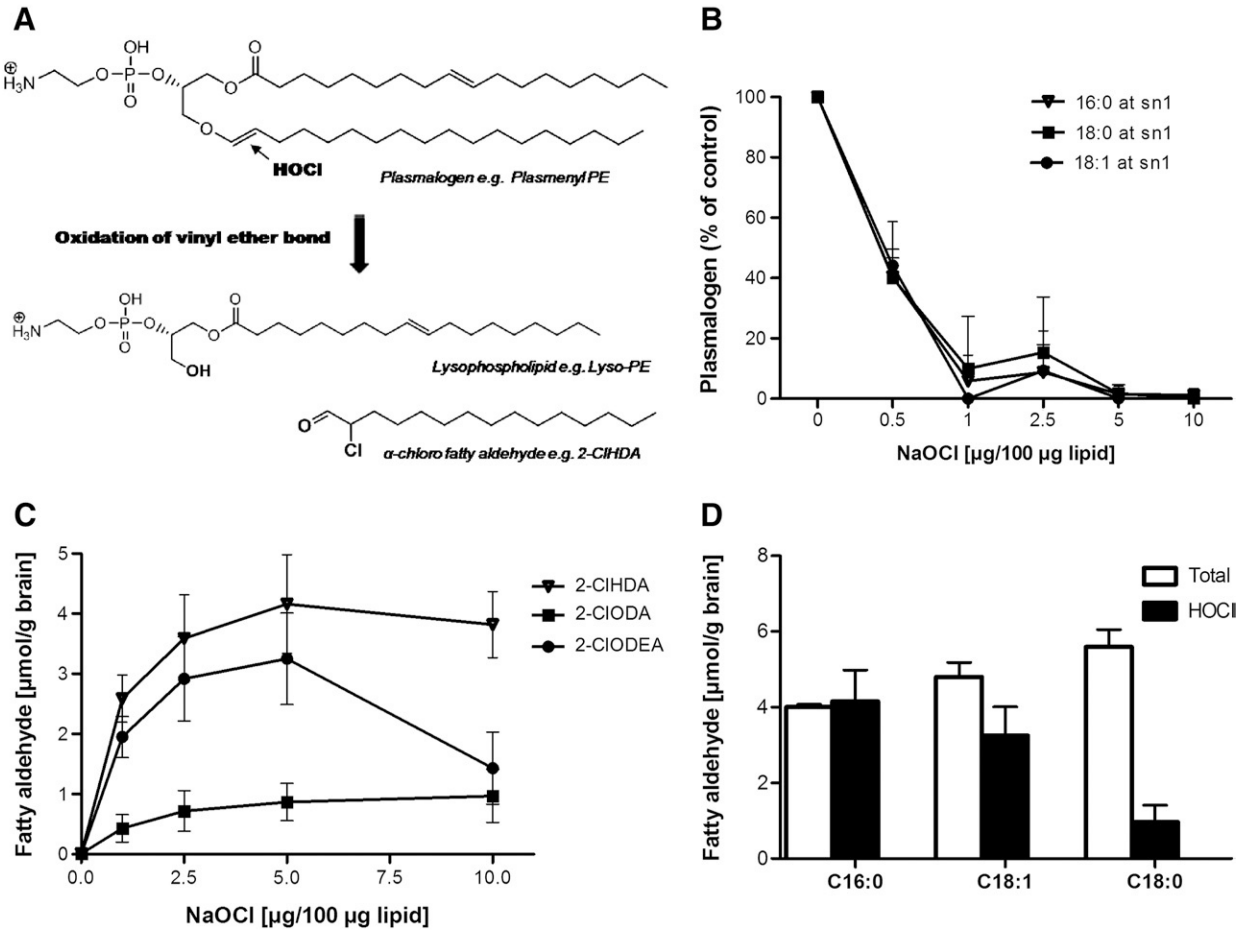

Fig. 3. HOCl modification of brain lipid extracts results in a decrease in selected pPE species and concomitant formation of the corresponding 2-chloro fatty aldehydes in vitro.

(A) Reaction pathway leading to the formation of 2-ClHDA and the corresponding lysophospholipid. (B) MS/MS analysis of selected pPE subspecies containing 16:0, 18:0, and 18:1 at the *sn*-1 position modified in the presence of the indicated oxidant:lipid ratios (w/w). (C) NICI–GC–MS analysis of the corresponding 2-chloro fatty aldehydes in HOCl-modified mouse brain lipid extracts. 2-Cl[$^{13}C_8$]HDA was used as internal standard. 2-ClHDA, 2-chlorohexadecanal; 2-ClODA, 2-chlorooctadecanal; 2-ClODEA, 2-chlorooctadecenal. Data shown represent means±SD from triplicate determinations. (D) NICI–GC–MS analysis of total fatty aldehyde after an overnight hydrolysis step at room temperature using 0.1 M HCl (termed “Total”) and 2-chloro fatty aldehyde concentrations after NaOCl modification (termed “HOCl”) of mouse brain lipid extracts.

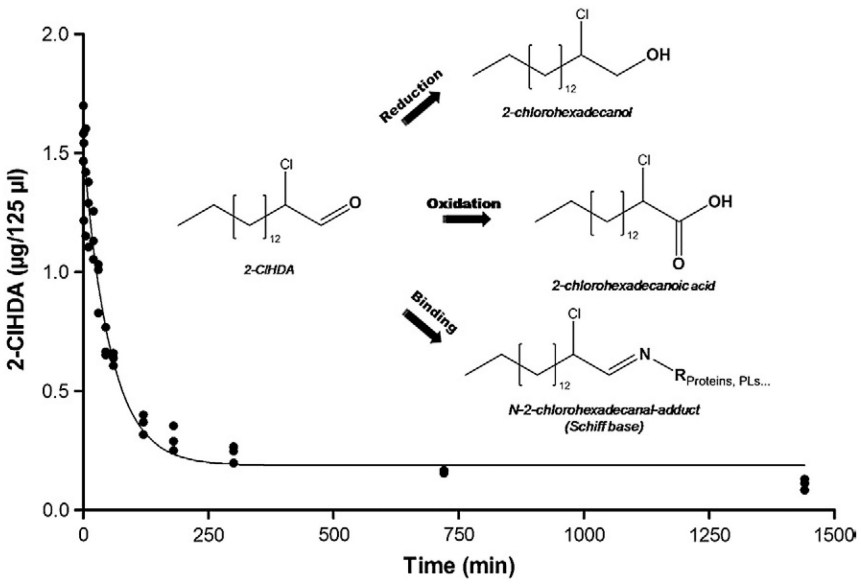

Fig. 4. Stability of 2-ClHDA in mixed primary mouse brain cell suspension.

Mixed brain cell suspensions prepared from three mouse brains in HBSS (supplemented with glucose; 1 g/L) were spiked with 2-ClHDA (stock added in DMSO; 30 µM final concentration). At the indicated times quantitative analysis of 2-ClHDA was performed by NICI–GC–MS using 2-Cl[$^{13}C_8$]HDA as internal standard. Experimental data were fitted by nonlinear regression analysis (R^2=0.96) as described under Materials and methods. The inset displays potential decay pathways for 2-ClHDA.

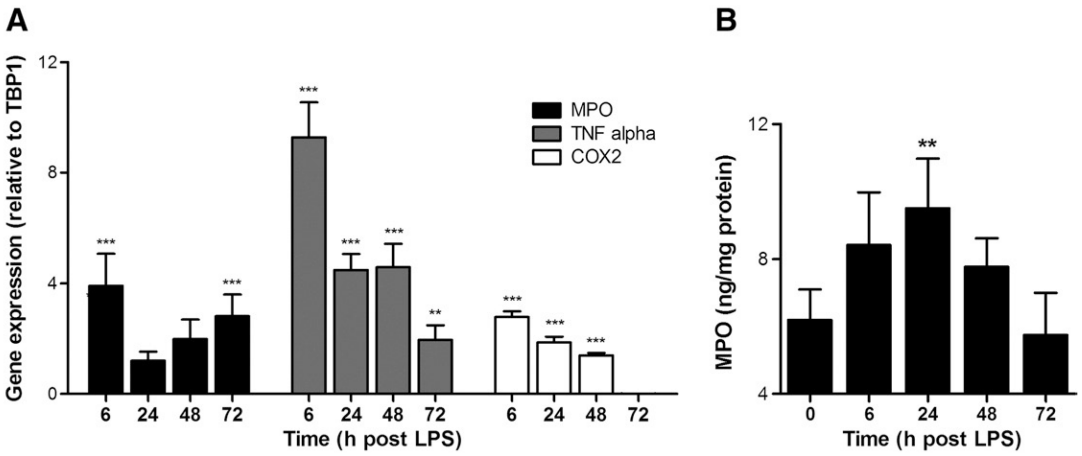

Fig. 5. Systemic LPS induces upregulation of brain inflammatory markers in vivo.

Eight-week-old male C57BL/6 mice received systemic LPS (150 μg/30 g; ip) at time 0. At the indicated time points animals were killed by cervical dislocation, brains were removed, and total brain RNA was isolated and reverse transcribed. cDNA was amplified using the primer pairs/assays described in Table 1. For ELISA measurements murine brain homogenates were used. (A) Relative gene expression of target genes is presented in relation to TBP1. Gene expression ratios were calculated by REST as described under Materials and methods (***$p \leq 0.001$; **$p \leq 0.01$). Results shown represent means±SD of four animals per time point. (B) Time-dependent accumulation of MPO protein in brain of LPS-treated mice as determined by ELISA. Results shown represent means±SD of four animals per time point (**$p < 0.01$).

Europe PMC Funders Author Manuscripts

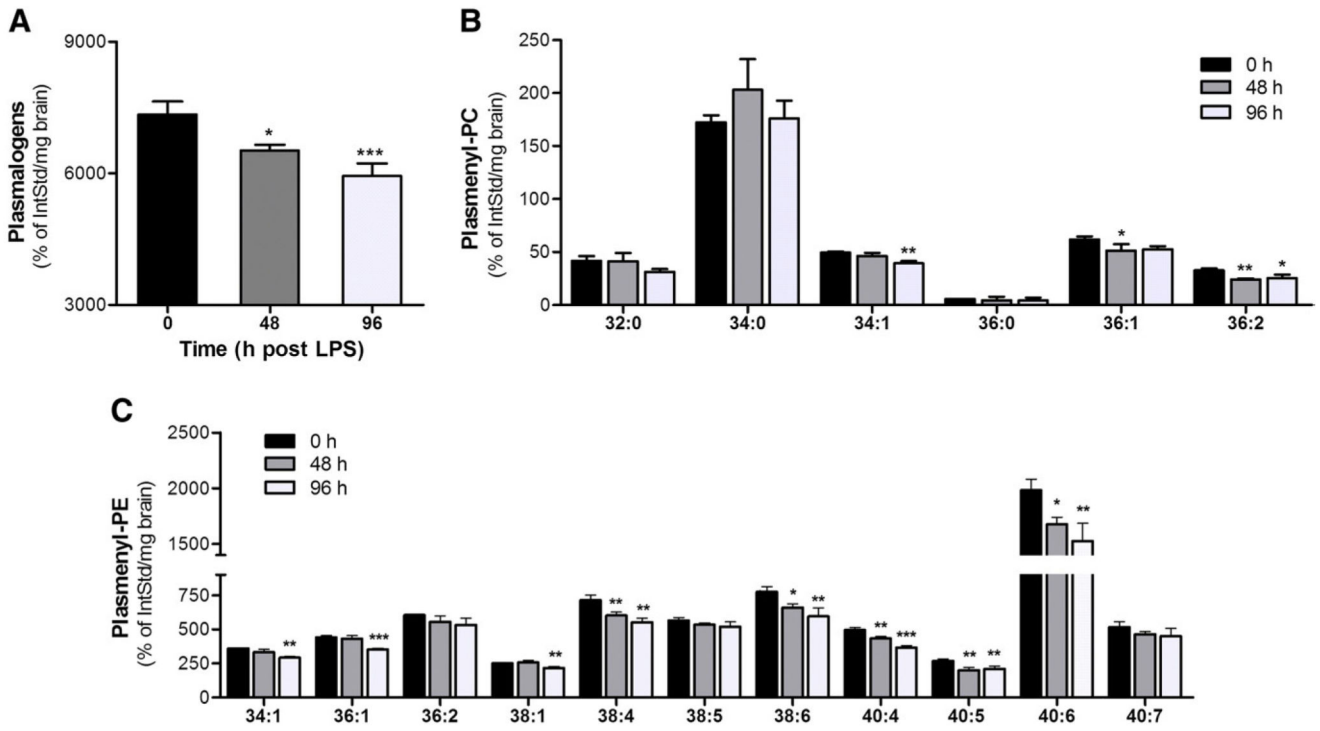

Fig. 6. Systemic LPS decreases plasmalogen levels in vivo.

Eight-week-old male C57BL/6 mice received systemic LPS (150 μg/30 g; ip) at time 0. At the indicated time points animals were killed by cervical dislocation, brains were removed, and lipids were extracted and analyzed by FT–ICR–MS using d_{31}-34:1 PC as internal standard. Data are given in terms of (A) total plasmalogens (sum of pPE and pPC) and (B) pPC and (C) pPE subspecies. Results shown represent means±SD of three animals per time point (*p<0.05; **p<0.01; ***p<0.001).

Europe PMC Funders Author Manuscripts

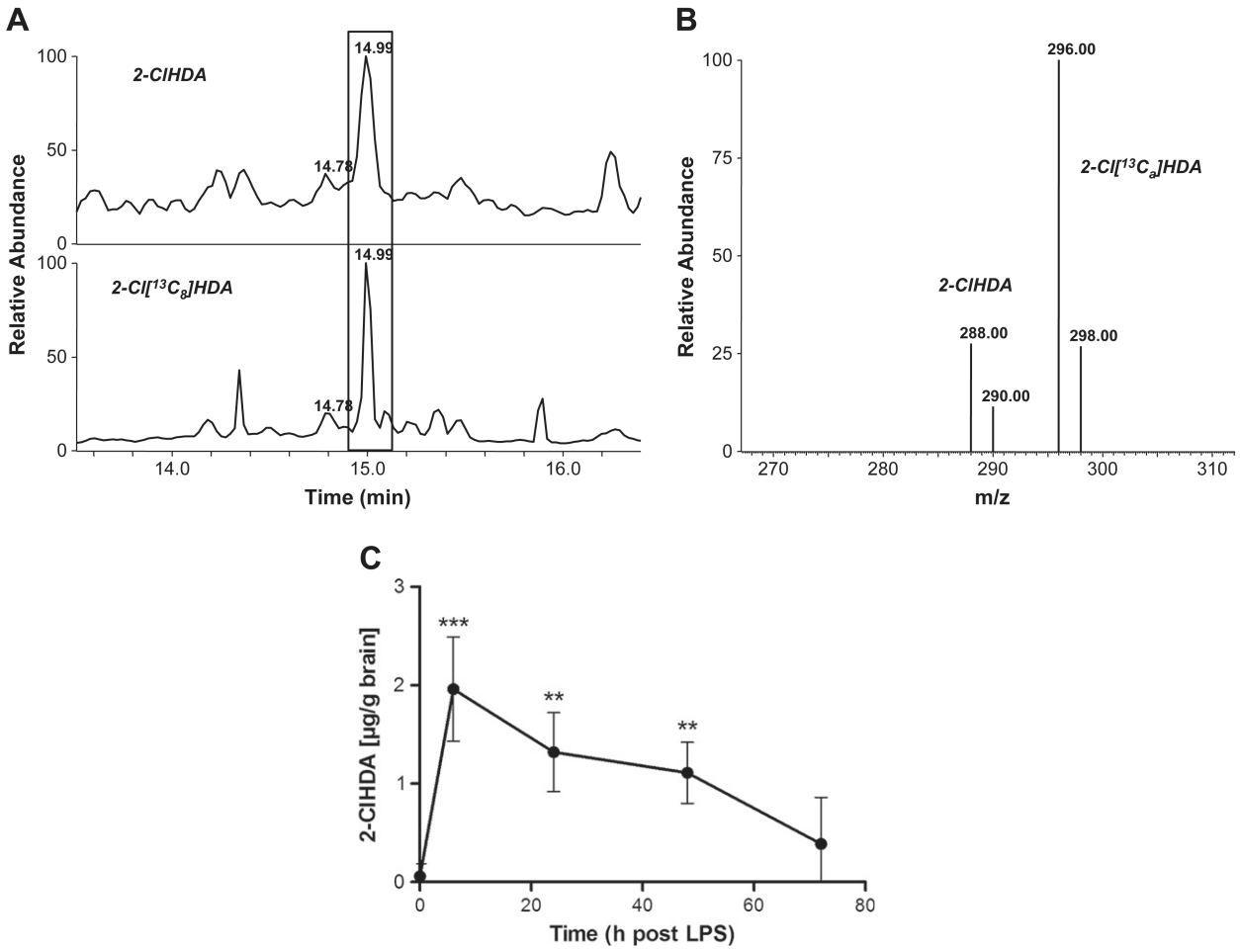

Fig. 7. Systemic LPS induces cerebral 2-ClHDA formation in vivo.

C57BL/6 mice received a single systemic LPS injection (150 µg/30 g; ip) at time 0. At the time points indicated, animals were killed by cervical dislocation, brains were removed, and lipids were extracted, preseparated by TLC, extracted from the plates, and converted to the corresponding PFB–oxime derivatives. 2-ClHDA concentrations were quantified by selected ion monitoring NICI–GC–MS analysis using 2-Cl[$^{13}C_8$]HDA as internal standard. (A) Selected ion monitoring of a representative brain lipid sample (top; 6 h post-LPS injection; *m/z*=288) and the internal standard (bottom; *m/z*=296). Boxed area indicates position of 2-ClHDA and 2-Cl[$^{13}C_8$]HDA. (B) Fragment ion intensity ratios of 2-ClHDA (*m/z*=288, 290) and the internal standard (*m/z*=296, 298) of the peak highlighted in (A). (C) Time-dependent formation of 2-ClHDA in brains of mice receiving a single systemic LPS dose. Results shown represent means±SD from four different animals per time point (**p<0.01; ***p<0.001 compared to time 0).

Europe PMC Funders Author Manuscripts

Table 1

Primer sequences used in this study

Target gene	Primer position	Sequence	Amplicon size (bp)
MPO, NM_010824.2	Forward	5′-GCCAGCAGCCATGAAGAAGT-3′	304
MPO, NM_010824.2	Reverse	5′-CCGGATCTCATCCACCACAA-3′	
TNFα, NM_013693	–	QT00104006, Qiagen	112
COX2, NM_011198	–	QT00165347, Qiagen	95
TBP1, NM_013684	–	QT00198443, Qiagen	114